Delamination Buckling and Growth in a Clamped Circular Plate

W.-L. Yin*
Georgia Institute of Technology, Atlanta, Georgia
and
Z. Fei†
Northern Jiaotung University, Beijing, China

The paper presents an elastic postbuckling analysis of a delaminated circular plate under axisymmetric compression along its clamped boundary. Von Kármán's equations are assumed to govern the deformation of the delaminated layer, while the deflection of the main body of the plate is described by the linear equations of the classical plate theory. Solution of the boundary-value problem is reduced to repeated numerical integration of two initial-value problems. Certain features of the postbuckling behavior are found to be qualitatively similar to the buckling of an axially loaded beam plate containing a one-dimensional delamination. An analytical expression of the energy-release rate is obtained in terms of the postbuckling solution. The stability of delamination growth under a fixed boundary displacement is examined. The results are compared with the previous results for thin-film circular delamination.

Nomenclature

a = radius of the delamination
$\bar{a}$ = $\{12(1-\nu^2)\epsilon_0\}^{1/2}a/h$
D_i = bending stiffnesses
E = Young's modulus
$f(\xi)$ = $\{6(1-\nu^2)\}^{1/2}w_1'(\xi)/h$
G = energy-release rate
$\bar{G}$ = $GR^4/(Et^5)$
h = thickness of the delamination
H = $t-h$
M_i = bending moments
$\bar{M}_i$ = $\{6(1-\nu^2)\}^{1/2}(a^2/hD_i)M_i(a)$
P_i = compressive radial forces
$\bar{P}$ = $(R/3.8317)^2P_1(R)/D_1$
Q_i = a^2P_i/D_i
R = radius of the base plate
t = thickness of the base plate
$u_i(r)$ = radial displacement of region i
$w_i(\xi)$ = $W_i(r)$ $(i=1,2)$
$W_i(r)$ = transverse deflections $(i=1,2,3)$
α = a/R
ϵ^* = $\{12(1-\nu^2)\epsilon_0\}^{1/2}(R/h)$
ϵ_0 = $-u_1(R)/R$
ξ = r/a
λ = $(Q_2)^{1/2}$
ν = Poisson's ratio
$\psi(\xi)$ = $\{6(1-\nu^2)\}^{1/2}(a^2/hr)W_3'(r)$
τ = h/t

Presented as Paper 85-0832 as the AIAA 26th Structures, Structural Dynamics, and Materials Conference, Orlando, FL, April 15-17, 1985; received Oct. 1, 1986; revision received Sept. 9, 1987.

*Professor, School of Civil Engineering, Member AIAA.
†Associate Professor, Research Institute of Engineering Mechanics.

I. Introduction

AXISYMMETRIC buckling and the ensuing growth of a thin circular delamination in a thick plate under equal biaxial compression was first studied by Kachanov,[1] who used a delamination growth criterion in terms of a critical energy-release rate. Since his study was based on the linear postbuckling equations of the delaminated layer, the results are valid only if the compressive strain in the base laminate does not increase significantly beyond the critical strain for layer buckling. In a recent work, Yin[2] applied von Karman's nonlinear plate equations to study axisymmetric elastic postbuckling deformation of a thin-film circular deflamination. In a "thin-film analysis," one assumes the delaminated layer to be so thin (compared to the base laminate) that the buckling of the layer does not affect the deformation of the base laminate. It was shown that the totality of all axisymetric postbuckling solutions of various thin-film circular delaminations may be reduced to a one-parameter family of nondimensionalized solutions. The various solutions of this family were obtained by numerical integration and iteration. Furthermore, the energy-release rate associated with the growth of delamination was evaluated by the method of M-integral. Delamination growth under a fixed laminate load was found to be an unstable process because the energy-release rate increases monotonically with the delamination radius.

By ignoring the bending deformation and the nonuniformity of stretching deformation in the base laminate due to the buckling of the delaminated layer, the thin-film analysis yields a relatively simple procedure for obtaining approximate postbuckling solutions. Nevertheless, previous study of a one-dimensional delamination by Chai et al.[3] indicated that the thin-film analysis may deliver solutions with significant underestimation of the energy-release rate. Consequently, it is desirable to undertake a more refined analysis of the circular delamination by taking into account buckling-induced deformation of the base laminate.

The improved analysis presented in this paper assumes that the ratio of the thickness of the delamination to that of the base plate is small but not negligible. Bending and nonuniform stretching deformation both occur in the base plate as

soon as the delamination buckles, but the bending deformation of the base plate remains relatively small compared to the corresponding deformation of the buckled layer because the base plate has a much larger bending stiffness. Although the postbuckling deformation of the thin layer is governed by von Kármán's nonlinear plate equations, the deformation in the base plate may be adequately described by the linear equations of the classical theory of plates. Based on the present assumption, we formulate the boundary-value problem of axisymmetric postbuckling deformation of a delaminated circular plate in Section II. In Section III, the task of obtaining the solutions of the boundary-value problem is reduced to repeated integration of two initial-value problems and to successive iterations. This shooting procedure delivers various families of postbuckling solutions, with each family corresponding to a particular ratio of the plate radius to the delamination radius. Shortly after the onset of buckling, the postbuckling deformation changes from an initial phase to a secondary phase with a distinctively different pattern of deformation. In the final section, we evaluate the energy-release rate by the method of M-integral, and examine the change of the energy-release rate with either an increasing inward boundary displacement or an increasing delamination radius. The relation is found to be monotone in the first case but not in the other case. Compared to the results of thin-film analysis, the energy-release rates obtained in the present study are generally greater except when the delamination growth approaches the fixed boundary of the base laminate, and in many cases the discrepancies may be very significant.

II. Formulation of the Problem

Figure 1 shows a clamped homogeneous isotropic circular plate of radius R containing a concentric circular delamination of radius a. The delamination separates the central portion of the plate into two layers (regions 2 and 3) of thickness H and h, respectively, where $H \gg h$. The remaining portion (region 1, $a \le r \le R$) has the thickness $t = H + h$. The critical radial compressive force that is required to initiate buckling of the delaminated plate has been obtained elsewhere[4] for any arbitrary combination of the radius ratio ($\alpha \equiv a/R$) and the thickness ratio ($\tau = h/t$). In the postbuckling states, each of the three regions ($i = 1,2,3$) undergoes radial displacement $u_i(r)$ and upward deflection $W_i(r)$. Since the thickness of region 3 is small compared to the remaining portions, W_3 is expected to be large compared to W_1 and W_2, provided that $\tau/\alpha \le 1$. (The postbuckling solutions of axially loaded beam plates with across-the-width delaminations demonstrate the validity of the statement in the case of one-dimensional delaminations.[5]) Consequently, we assume that the deflection functions $W_1(r)$ and $W_2(r)$ are governed by the linear postbuckling equations of the classical plate theory, whereas the deflection $W_3(r)$ is governed by von Kámán's nonlinear equations. Let $P_1(r)$, P_2, and $P_3(r)$ denote the radial compressive force per unit circumferential arc length in regions 1, 2, and 3, respectively; P_2 is independent of the radial coordinate because region 2 is a circular plate undergoing small postbuckling deflection. We introduce the dimensionless quantities

$$\xi = r/a, \qquad \tau = h/t, \qquad \alpha = a/R$$
$$Q_i(\xi) = P_i(r)\,a^2/D_i, \qquad i = 1,3$$
$$\lambda^2 = Q_2 = P_2 a^2/D_2 \tag{1}$$

where

$$D_1 = Et^3/\{12(1-\nu^2)\}, \quad D_2 = (1-\tau)^3 D_1$$
$$D_3 = \tau^3 D_1 \tag{2}$$

Furthermore, we let

$$\psi(\xi) = \{6(1-\nu^2)\}^{1/2}(a^2/hr)\,W_3'(r)$$
$$w_i(\xi) = W_i(r), \qquad i = 1,2 \tag{3}$$

Then the following system of governing equations for region 3 may be obtained from von Karman's theory.[2,6]

$$\xi^{-3}\{\xi^3 Q_3'(\xi)\}' = \psi(\xi)^2$$
$$\xi^{-3}\{\xi^3 \psi'(\xi)\}' = -Q_3(\xi)\psi(\xi) \qquad (0 \le \xi \le 1)$$
$$Q_3'(0) = 0, \qquad \psi'(0) = 0 \tag{4}$$

where the prime indicates differentiation with respect to ξ.

The system given by Eq. (4) together with any specified pair of initial values $\psi_o = \psi(0)$ and $Q_o = Q_3(0)$ constitute an initial value problem whose unique solution can be obtained by numerical integration. The slope of the profile and the radial displacement at $r = a$ may be expressed in terms of the boundary values of the solution, namely,

$$\left.\frac{dW_3}{dr}\right|_{r=a} = \frac{h\psi(1)}{a\{6(1-\nu^2)\}^{1/2}}$$
$$u_3(a) = -\frac{Q_3'(1) + (1-\nu)Q_3(1)}{12(1-\nu^2)\,a/h^2} \tag{5}$$

The preceding expression for $u_3(a)$ has been derived elsewhere [see Eqs. (5) and (16) of Ref. 2].

The linear differential equation governing the transverse deflection in region 2

$$[\xi^{-1}\{\xi w_2'(\xi)\}']' = -\lambda^2 w_2'(\xi)$$

has the following solution

$$w_2(\xi) = B_1 J_0(\lambda\xi) + B_2$$

Hence

$$\left.\frac{dW_2}{dr}\right|_{r=a} = (1/a)\,w_2'(1) = -(B_1\lambda/a)\,J_1(\lambda)$$

This expression must agree with Eq. (5) because of the continuity of the slope at $r = a$. Consequently,

$$w_2'(\xi) = -B_1\lambda J_1(\lambda\xi), \quad B_1 = \frac{h\psi(1)}{\{6(1-\nu^2)\}^{1/2}\lambda J_1(\lambda)} \tag{6}$$

The membrane stresses, strains, and the boundary radial displacement of region 2 are

$$\sigma_r = \sigma_\theta = -P_2/H, \qquad \epsilon_r = \epsilon_\theta = -(1-\nu)\,P_2/(EH)$$
$$-u_2(a) \approx (1-\nu)\,P_2 a/(EH)$$

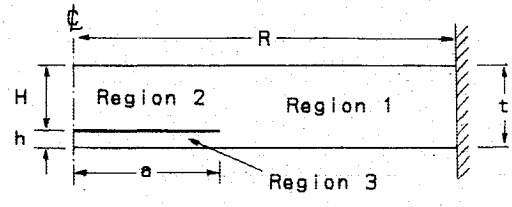

Fig. 1 Circular delamination model.

We require the compatibility of the radial displacements at $r = a$ for regions 2 and 3, i.e.,

$$u_3(a) = u_2(a) + \frac{h+H}{2}\frac{\mathrm{d}W_3}{\mathrm{d}r}\bigg|_a$$

This yields the value of the parameter λ, hitherto undetermined, i.e.,

$$\lambda^2 = \frac{P_2 a^2}{D_2} = \left(\frac{\tau}{1-\tau}\right)^2\left\{\frac{Q_3'(1)}{1-\nu} + Q_3(1)\right\} + \frac{\tau}{(1-\tau)^2}\left\{\frac{6(1+\nu)}{1-\nu}\right\}^{1/2}\psi(1) \tag{7}$$

We now formulate the equations governing region 1. The transverse deflection in this region satisfies the equation

$$\left[\xi^{-1}\{\xi w_1'(\xi)\}'\right] = -Q_1(\xi)w_1'(\xi), \qquad 1 \le \xi \le 1/\alpha$$

We let

$$f(\xi) \equiv \{6(1-\nu^2)\}^{1/2} w_1'(\xi)/h \tag{8}$$

Then

$$\left[\xi^{-1}\{\xi f(\xi)\}'\right]' = -Q_1(\xi)f(\xi), \qquad 1 \le \xi \le 1/\alpha$$
$$f(1) = \psi(1) \tag{9}$$

where the last condition follows from the continuity of the slope at $r = a$. The membrane stresses in region 1 are given by

$$\sigma_r(r) = A_1 - A_2 r^{-2}, \qquad \sigma_\theta(r) = A_1 + A_2 r^{-2}$$

The coefficients A_1 and A_2 may be determined as follows. First, the circumferential membrane strain at $r = a$ is given by

$$u_1(a)/a = (1-\nu)A_1/E + (1+\nu)A_2/(Ea^2)$$

Using the compatibility condition

$$u_1(a) = u_2(a) + (h/2)W_3'(a)$$

and the solution in region 2, we find that

$$(1-\nu)a^2A_1 + (1+\nu)A_2 = \frac{Eh^2\psi(1)}{2\{6(1-\nu^2)\}^{1/2}} - \frac{1-\nu}{H}D_2\lambda^2$$
$$= -(1/t)(1-\nu)\{D_2\lambda^2 + D_3Q_3(1)\} - (1/t)D_3Q_3'(1)$$

where Eq. (7) was used to obtain the last expression. Next, from Fig. 2a we obtain the equilibrium equation $P_1 = P_2 + P_3$ at $r = a$, or

$$\sigma_r|_{r=a} = A_1 - A_2/a^2 = -\{D_2\lambda^2 + D_3Q_3(1)\}/(ta^2)$$

Solving the preceding two equations for A_1 and A_2, we obtain

$$A_1 = -\{Q_3'(1)D_3/2 + D_3Q_3(1) + D_2\lambda^2\}/(ta^2)$$
$$A_2 = -D_3Q_3'(1)/(2t)$$

Consequently,

$$Q_1(\xi) = (1-\tau)^3\lambda^2 + \tau^3\left[Q_3(1) + (1-1/\xi^2)Q_3'(1)/2\right] \tag{10}$$

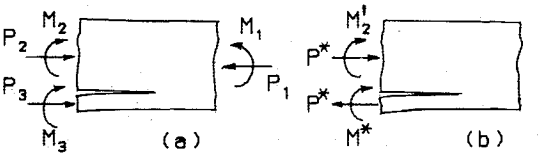

Fig. 2 Forces and moments along the crack boundary.

Along the exterior boundary of region 1, we have

$$Q_1(R/a) = (1-\tau)^3\lambda^2 + \tau^3\left[Q_3(1) + (1-a^2/R^2)Q_3'(1)/2\right] \tag{11}$$

and

$$u_1(R) = R\epsilon_\theta(R) = (R/E)\{(1-\nu)A_1 + (1+\nu)A_2/R^2\}$$
$$= -\frac{R\tau}{12(1+\nu)}\left(\frac{h}{a}\right)^2\left[Q(1) + (1/\tau - 1)^3\lambda^2 + \left(1 + \frac{1+\nu}{1-\nu}\frac{a^2}{R^2}\right)Q_3'(1)/2\right] \tag{12}$$

Finally, we consider the radial bending moment per unit circumferential arc length near the delamination boundary in each of the three regions 1, 2, and 3. We have

$$M_1(a) = D_1\{W_1''(r) + (\nu/r)W_1'(r)\}|_{r=a}$$
$$= \{6(1-\nu^2)\}^{-1/2}(D_1h/a^2)\{f'(1) + \nu\psi(1)\}$$
$$M_2(a) = \{6(1-\nu^2)\}^{-1/2}(D_2h/a^2)\psi(1) \times \{1 + \nu - \lambda J_2(\lambda)/J_1(\lambda)\}$$
$$M_3(a) = \{6(1-\nu^2)\}^{-1/2}(D_3h/a^2) \times \{\psi'(1) + (1+\nu)\psi(1)\} \tag{13}$$

Substituting the preceding expressions into the equilibrium equation of moments

$$M_1(a) = M_2(a) + M_3(a) + P_2h/2 - P_3(a)H/2$$

we obtain an expression of $f'(1)$ in terms of the boundary values (at $\xi = 1$) of the solutions of regions 2 and 3. This expression together with Eqs. (7), (9), and (10) define the following initial-value problem for the function $f(\xi)$:

$$\left[\xi^{-1}\{\xi f(\xi)\}'\right]' = -f(\xi)\left\{(1-\tau)^3\lambda^2 + \tau^3Q_3(1) + \tau^3(1-\xi^{-2})Q_3'(1)/2\right\}, \qquad 1 \le \xi \le R/a \tag{14a}$$

$$f(1) = \psi(1) \tag{14b}$$

$$f'(1) = -\nu\psi(1) + (1-\tau)^3\psi(1)\{1 + \nu - \lambda J_2(\lambda)/J_1(\lambda)\} + \tau^3\{\psi'(1) + (1+\nu)\psi(1)\} + \{6(1-\nu^2)\}^{1/2}\left\{(1-\tau)^3\lambda^2 - (1-\tau)\tau^2Q_3(1)\right\}/2 \tag{14c}$$

where λ^2 is given by Eq. (7).

III. Postbuckling Solutions

If all material and geometrical parameters are given, then, for any specified pair of numbers Q_o and ψ_o, the following nonlinear initial-value problem

$$\xi^{-3}\{\xi^3 Q_3'\}' = \psi^2, \quad \xi^{-3}\{\xi^3\psi'\}' = -Q_3\psi, \quad 0 \le \xi \le 1$$

$$Q_3'(0) = \psi'(0) = 0, \quad Q_3(0) = Q_o, \quad \psi(0) = \psi_o \quad (15)$$

has a unique solution $\{\psi(\xi), Q_3(\xi)\}$. Substituting the final values $\psi(1)$, $Q_3(1)$, $\psi'(1)$, and $Q_3'(1)$ into Eqs. (7) and (14), and solving the initial-value problem of Eq. (14), one obtains the function $f(\xi)$ in the interval $1 \le \xi \le R/a$. This solution generally does not satisfy the clamped condition $f(R/a) = 0$ at the exterior boundary (i.e., the condition $dW_1/dr = 0$ at $r = R$). Therefore, for any specified Q_o, one must search ψ_o iteratively until successive integration of Eqs. (14) and (15) delivers a solution $f(\xi)$ satisfying $f(R/a) = 0$. For a different choice of Q_o, this shooting procedure selects another ψ_o which yields a new solution. Hence, a one-parameter family of postbuckling solutions can be obtained depending on the value of the parameter Q_o. This parameter is related to the radial membrane compression and the radial displacement at the exterior boundary, given, respectively, by Eqs. (11) and (12).

Extending the procedure of Ref. 2, we integrate Eqs. (14) and (15) numerically at each step of the iteration process by using the fourth-order Runge-Kutta formula. The thickness ratio $h/t = 0.1$ is selected so as to represent a moderately thin delamination, and Poisson's ratio is chosen to be 0.3. For each selected value of R/a, we implement the shooting procedure to obtain a sequence of postbuckling solutions. Each individual solution of the sequence is based on a particular choice of Q_o, and the postbuckling deformation described by that solution may be produced by applying the appropriate boundary compression or boundary displacement as given, respectively, by Eqs. (11) and (12). Since the present analysis assumes small deflection in the base plate and relatively large deflection in the delaminated layer, and since this assumption cannot be valid if $a/R < h/t$, no attempt is made to obtain solutions for the case $R/a > 10$. For $R/a < t/h = 10$, however, the delaminated layer has a smaller thickness-to-radius ratio compared to the base plate. Consequently, buckling of the plate can be initiated by local buckling of the delaminated layer at a critical edge load significantly below the corresponding critical load of a perfect plate without delamination.[4] Hence, there is a range of applied loads (between the two critical loads) such that the pattern of deformation of the delaminated plate conforms to the assumptions of the present analysis. The values of R/a used in this work to obtain numerical solutions vary from 1.1 to 10.

In view of Eq. (13), we introduce the dimensionless moments

$$\overline{M}_i = \{6(1-\nu^2)\}^{1/2}(a^2/hD_i)M_i(a), \qquad i = 1,2,3$$

Then

$$\overline{M}_1 = f'(1) + \nu\psi(1)$$

$$\overline{M}_2 = \psi(1)\{1 + \nu - \lambda J_2(\lambda)/J_1(\lambda)\}$$

$$\overline{M}_3 = \psi'(1) + (1+\nu)\psi(1)$$

From Eq. (5) and

$$\frac{M_i(a)}{D_i} = \left(\frac{d^2W_i}{dr^2} + \frac{\nu}{r}\frac{dW_i}{dr}\right)\Bigg|_{r=a}$$

we obtain

$$\overline{M}_i - \nu\psi(1) = \{6(1-\nu^2)\}^{1/2}(a^2/h)(d^2W_i/dr^2)\big|_{r=a}$$

Hence, $\overline{M}_i - \nu\psi(1)$ is proportional to the meridional curvature of the middle surface of region i at $r = a$. The meridional tangent lines of the three middle surfaces have the same slope $(h/a)\{6(1-\nu^2)\}^{-1/2}\psi(1)$ at $r = a$. In each family of postbuckling solutions corresponding to a given value of R/a, both the radial compression and the inward radial displacement at $r = R$ increase monotonically with decreasing $Q_3(0)$, while $\psi(1)$ at first increases and then decreases monotonically. [see Tables 1 and 2 for the main features of two families of solutions corresponding to $R/a = 8$ and 4, respectively. The decrease of $\psi(0)$ occurs at a high level of boundary compression exceeding that corresponding to the last solutions of Tables 1 and 2.] At the transition state of postbuckling deformation when $\psi(1)$ changes from positive to negative, we have $w_2'(\xi) \equiv 0$ as implied by Eq. (6). Hence, region 2 suffers no bending deformation in the transition state. Furthermore, Eqs. (14a) and the boundary conditions $f(R/a) = 0$ and $f(1) = \psi(1) = 0$ define an eigenvalue problem for the function $f(\xi)$ in the interval $1 \le \xi \le R/a$. The eigenvalue problem has a nontrivial solution only if the boundary load $P_1(R)$ reaches the critical load for the buckling of the annular plate $a \le r \le R$ with vanishing slope along inner and outer boundaries. But the transition state $\psi(1) = 0$ follows shortly the local buckling of the delaminated layer when the boundary load $P_1(R)$ is relatively small. Hence, at that instant the boundary-value problem of Eq. (14a) and $f(1) = f(R/a) = 0$ has the trivial solution $f(\xi) \equiv 0$. Thus, region 1 also suffers no bending deformation in the transition state and only region 3 undergoes transverse deflection. A similar transition state of postbuckling deformation has been found in the case of an axially loaded beam plate containing a relatively thin and long one-dimensional delamination.[5]

The transition state divides the postbuckling process into two successive phases (Fig. 3). In the initial phase that immediately follows buckling, all three regions of the plate deflect downward. The entire middle surface of region 2 and a central portion of the delaminated layer are concaved upward, while a boundary portion of the delaminated layer and the entire middle surface of region 1 are concaved downward. In the secondary phase following the transition, regions 1 and 2 deflect upward and reverse their respective directions of concavity, while the central portion of the delaminated layer continues its downward deflection. The separation between

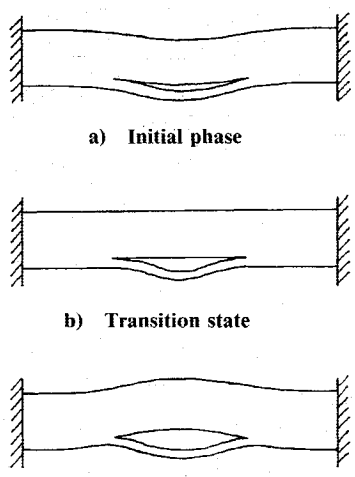

a) Initial phase

b) Transition state

c) Secondary phase

Fig. 3 Two phases of postbuckling deformation.

Table 1 Postbuckling solutions and energy-release rates ($\nu = 0.3$, $h/t = 0.1$, $R/a = 8$)

$\psi(0)$	$Q_3(0)$	$\psi(1)$	$Q_3(1)$	$\bar{M}_1$	$\bar{M}_2$	$\bar{M}_3$	$\bar{P}$	$\bar{a}$	$\bar{G}$
0.889	14.650	0.00028	14.686	−0.00011	0.00034	−0.717	0.6416	3.2098	0.000177
1.713	14.600	0.00025	14.735	−0.00009	0.00029	−1.385	0.6464	3.2219	0.000660
2.647	14.500	−0.00012	14.824	0.00004	−0.00013	−2.151	0.6551	3.2436	0.001596
4.108	14.250	−0.00146	15.037	0.00051	−0.00141	−3.380	0.6758	3.2943	0.003959
5.150	14.000	−0.00306	15.246	0.00098	−0.00269	−4.289	0.6960	3.3432	0.006406
6.735	13.500	−0.0068	15.664	0.0018	−0.0051	−5.749	0.7361	3.4384	0.011608
7.981	13.000	−0.0112	16.087	0.0021	−0.0072	−6.983	0.7763	3.5311	0.017266
9.955	12.000	−0.0233	16.958	−0.0003	−0.0112	−9.156	0.8562	3.7085	0.030141
13.008	10.000	−0.1078	19.011	−0.0756	−0.0242	−13.248	0.9668	3.9412	0.064219
15.389	8.000	−0.2904	21.422	−0.2687	−0.0080	−17.350	0.9838	3.9761	0.110678
17.183	6.000	−0.4954	23.880	−0.4863	0.0597	−21.423	0.9877	3.9845	0.170122
18.581	4.000	−0.7183	26.424	−0.7224	0.1694	−25.630	0.9896	3.9888	0.246083
19.684	2.000	−0.9624	29.097	−0.9801	0.3142	−30.077	0.9908	3.9919	0.343062
20.552	−0.000	−1.2312	31.930	−1.2632	0.4894	−34.846	0.9917	3.9945	0.466702
21.222	−2.000	−1.5286	34.952	−1.5759	0.6910	−40.008	0.9926	3.9971	0.624140
21.611	−3.500	−1.7732	37.360	−1.8326	0.8572	−44.179	0.9933	3.9991	0.769761

Table 2 Postbuckling solutions and energy-release rates ($\nu = 0.3$, $h/t = 0.1$, $R/a = 4$)

$\psi(0)$	$Q_3(0)$	$\psi(1)$	$Q_3(1)$	$\bar{M}_1$	$\bar{M}_2$	$\bar{M}_3$	$\bar{P}$	$\bar{a}$	$\bar{G}$
0.934	14.650	0.00023	14.690	−0.00017	0.00029	−0.753	0.1604	3.2103	0.000012
1.723	14.600	0.00020	14.737	−0.00014	0.00024	−1.393	0.1616	3.2221	0.000042
2.645	14.500	−0.00010	14.824	0.00007	−0.00011	−2.149	0.1638	3.2436	0.000100
4.097	14.250	−0.00119	15.033	0.00083	−0.00115	−3.370	0.1689	3.2946	0.000246
5.134	14.000	−0.00245	15.239	0.00171	−0.00216	−4.276	0.1740	3.3441	0.000398
7.951	13.000	−0.0083	16.064	0.0056	−0.0054	−6.955	0.1946	3.5367	0.001072
9.901	12.000	−0.0150	16.907	0.0099	−0.0073	−9.102	0.2158	3.7255	0.001866
12.726	10.000	−0.0307	18.664	0.0190	−0.0075	−12.944	0.2611	4.0987	0.003891
14.781	8.000	−0.0500	20.533	0.0284	−0.0033	−16.681	0.3106	4.4715	0.006646
16.367	6.000	−0.0739	22.531	0.0378	0.0059	−20.550	0.3649	4.8477	0.010352
17.615	4.000	−0.1038	24.677	0.0461	0.0206	−24.686	0.4245	5.2293	0.015297
18.600	2.000	−0.1423	26.990	0.0516	0.0425	−29.187	0.4897	5.6171	0.021851
19.371	0.000	−0.1935	29.497	0.0508	0.0741	−34.147	0.5604	6.0097	0.030491
20.198	3.000	−0.3120	33.690	0.0215	0.1517	−42.648	0.6742	6.5933	0.048700
20.717	6.000	−0.5337	38.547	−0.0952	0.3009	−52.702	0.7852	7.1171	0.075419
21.067	−10.000	−1.1509	46.382	−0.5573	0.7173	−68.899	0.8857	7.5629	0.128837

regions 2 and 3 at $r = 0$ increases with the applied boundary compression, while the membrane compression at the center of the delaminated layer steadily decreases. The compression $Q_3(0)$ eventually attains negative values. That the membrane stress in the central portion of a circular plate changes from compression to tension at an advanced stage of axisymmetric postbuckling deformation has been remarked elsewhere.[6,7]

In Tables 1 and 2, $\bar{P}$ and $\bar{a}$ refer to the dimensionless quantities defined, respectively, in terms of the radial compressive load and inward radial displacement along the boundary $r = R$:

$$\bar{P} = \frac{P_1(R)}{(3.832/R)^2 D_1} = \frac{Q_1(R/a)}{(3.832\ a/R)^2} \tag{16}$$

$$\bar{a} = \left\{12(1-\nu^2)\epsilon_o\right\}^{1/2} a/h \tag{17}$$

where

$$\epsilon_o = -\epsilon_\theta(r) = -u_1(R)/R$$
$$= \frac{1}{12}\left(\frac{h}{a}\right)^2\left[\frac{\tau}{1+\nu}\left\{Q_3'(1)/2 + Q_3(1)\right.\right.$$
$$\left.\left.+\left(\frac{1-\tau}{\tau}\right)^3\lambda^2\right\} + \frac{\tau Q_3'(1)}{2(1-\nu)}\left(\frac{a}{R}\right)^2\right] \tag{18}$$

Here $\bar{P}$ is the ratio of the boundary load on the delaminated plate to the critical load of a perfect clamped circular plate without delamination. When $\bar{P}$ is not close to unity, significant bending deformation is localized in the delaminated layer and the deflection of the base plate is small.

Localized buckling changes into appreciable global buckling as $\bar{P}$ increases toward unity. In this process the radial membrane force in a central region of the delamination changes from compression to tension and the meridional curvature of the middle surface increases rapidly near the boundary of delamination. Hence, the radial bending moments and the energy-release rate also show dramatic increases as may be seen in the last few solutions of Tables 1 and 2. This boundary effect, associated with the postbuckling deformation of a flat plate under large membrane compression, has significant implications for the growth behavior of a two-dimensional delamination in contrast to that of a one-dimensional delamination.[2]

A basic assumption of the present work is that the buckling deformation of the base plate is small compared to that of the delaminated layer as well as to the thickness of the plate, so that linear governing equations may be justified in regions 1 and 2. The maximum deflections in the two regions are of the order

$$R\frac{\mathrm{d}w_i}{\mathrm{d}r}\bigg|_{r=a} = \frac{\psi(1)hR}{\left\{6(1-\nu^2)\right\}^{1/2} a}$$

The deflections are small compared to the plate thickness t if

$$\psi(1) \ll \{6(1-\nu^2)\}^{1/2} \frac{at}{Rh}$$

The condition is satisfied by all solutions presented in the tables and figures of the present work. An order-of-magnitude comparison of the deflections of the three regions may be made by examining the radial curvatures of their deformed middle planes at $r=a$. Discounting a common factor, these curvatures are given by $\overline{M}_i - \nu\psi(1)$. Tables 1 and 2 indicate that the boundary curvature of the delaminated layer is generally two or more orders greater than the curvatures of the base plate. Consequently, the use of linear governing equations may be justified for regions 1 and 2 when the thickness ratio is not smaller than the present value ($t/h=10$).

IV. The Energy-Release Rate and the Stability of Delamination Growth

Evaluation of the energy-release rate using the method of the M-integral essentially follows the procedure described in Ref. 2 for a thin-film circular delamination. However, in the present case the bending and membrane stresses in the base plate contribute to the M-integral. As in the study of a one-dimensional delamination,[8] we decompose the system of forces and moments in Fig. 2a into two subsystems.

$$M_i = M_i' + M_i'', \quad P_i = P_i' + P_i'', \quad i=1,2,3 \qquad (19)$$

The first subsystem $\{P_i', M_i'\}$ is defined by

$$\begin{aligned} &P_1'=0, \qquad P_2' = -P_3' = \tau\{P_1 - 6(1-\tau)M_1/t\} - P_3 \equiv P^* \\ &M_1'=0, \qquad M_3' = M_3 - M_1\tau^3 \equiv M^* \\ &M_2' = M_2 - M_1(1-\tau)^3 = P^*t/2 - M^* \end{aligned} \qquad (20)$$

and sketched in Fig. 2b. The second subsystem $\{P_i'', M_i''\}$ given by

$$\begin{aligned} &P'' = P_1, \qquad P_2'' = (1-\tau)P_1 + 6\tau(1-\tau)M_1/t \\ &P_3'' = \tau P_1 - 6\tau(1-\tau)M_1/t \\ &M_1'' = M_1, \qquad M_2'' = (1-\tau)^3 M_1, \qquad M_3'' = \tau^3 M_1 \end{aligned}$$

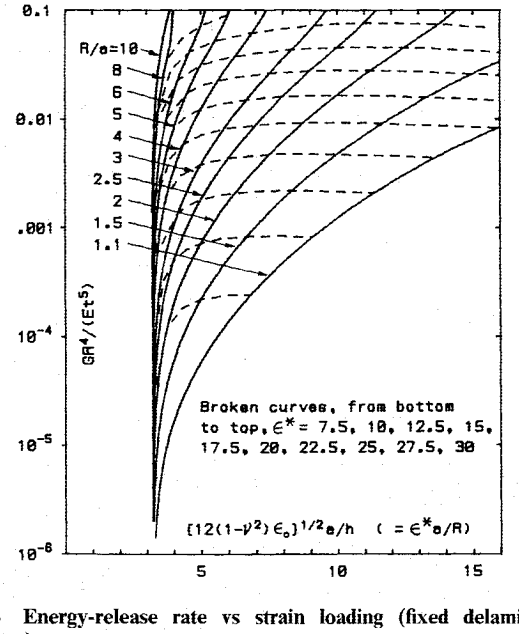

Fig. 4 Energy-release rate vs strain loading (fixed delamination geometry).

produces a nonsingular stress field near the delamination boundary $r=a$:

$$\sigma_r = -P_1/t - 12M_1\eta/t^3, \qquad -t/2 \le \eta \le t/2$$

where η is the coordinate normal to the middle surface. Consequently, the energy-release rate depends only on the first subsystem of loading. When the second subsystem is removed by superimposing an opposite system, region 1 of the plate ($1 \le \xi \le 1/\alpha$) becomes stress free (except in the vicinity of the delamination boundary). Hence, $u_1(a) = u_1'(a) = 0$ and the continuity of the radial displacement requires that $u_2(a) = u_3(a) = 0$. Thus, in regions 2 and 3 near $r=a$, we have $\epsilon_\theta = 0$ and consequently

$$\epsilon_r = \frac{1-\nu^2}{E}\sigma_r$$

The energy-release rate can be obtained by evaluating the M-integral over a surface $\mathcal{S}$ enclosing the delamination boundary

$$\begin{aligned} M &= \iint_{\mathcal{S}} \left(Wx_i n_i - \sigma_{jk} n_k u_{j,i} x_i - \sigma_{ik} n_k u_i\right) \mathrm{d}A \\ &= \frac{2\pi a^2}{2E}(1-\nu^2)\left[\int_{-h/2}^{h/2} \sigma_r^2\Big|_{\text{region 3}} \mathrm{d}\eta + \int_{-H/2}^{H/2} \sigma_r^2\Big|_{\text{region 2}} \mathrm{d}\eta\right] \\ &= \frac{\pi a^2(1-\nu^2)}{E}\left[\int_{-h/2}^{h/2}\left(\frac{P^*}{h} + \frac{12M^*}{h^3}\eta\right)^2 \mathrm{d}\eta \right. \\ &\quad \left. + \int_{-H/2}^{H/2}\left(\frac{P^*}{H} + \frac{P^*t/2 - M^*}{H}12\eta\right)^2 \mathrm{d}\eta\right] \\ &= \frac{\pi a^2(1-\nu^2)}{Eh}\left[\frac{P^{*2}}{1-\tau} + 12\left(\frac{M^*}{h}\right)^2 \right. \\ &\quad \left. + 12\frac{\tau}{(1-\tau)^3}\left(\frac{P^*}{2} - \frac{\tau M^*}{h}\right)^2\right] \end{aligned}$$

Since the energy-release rate G is given by[2]

$$G = M/(2\pi a^2)$$

we have

$$\overline{G} \equiv \frac{GR^4}{Et^5} - \frac{1-\nu^2}{2}\left[\frac{\beta_1}{\tau(1-\tau)} + \frac{12}{\tau^3}\beta_2 + \frac{12}{(1-\tau)^3}\beta_3\right] \qquad (21)$$

where

$$\begin{aligned} \beta_1 &\equiv \{12(1-\nu^2)\alpha^2\}^{-2} \\ &\times\left[\tau Q_1(1) - \frac{6\tau^2(1-\tau)\{f'(1) + \nu\psi(1)\}}{\{6(1-\nu^2)\}^{1/2}} - \tau^3 Q_3(1)\right]^2 \\ \beta_2 &\equiv \{12(1-\nu^2)\alpha^2/\tau^4\}^{-2} \\ &\times[\psi'(1) + \psi(1) - f'(1)]^2/\{6(1-\nu^2)\} \\ \beta_3 &\equiv \left(\beta_1^{1/2} - \beta_2^{1/2}\right)^2 \end{aligned}$$

Equation (21) is used to compute the normalized energy-release rates associated with the postbuckling solutions and the results are shown in the last columns of Tables 1 and 2 for the cases $R/a=8$ and 4. Although the postbuckling solutions for other values of R/a are not tabulated in the present

paper, the dependence of $\bar{G}$ upon $\bar{a}$ for such solutions are shown by the solid curves in Fig. 4. The curves indicate that, if the delamination radius does not change (R/a = constant), then the energy-release rate increases monotonically with the boundary displacement

$$-u_1(R) = R\epsilon_o \equiv \bar{a}^2 h^2 R/\{12(1-\nu^2)a^2\}$$

If we assume a delamination growth criterion based on a critical value of the total energy-release rate without discriminating between its mode I and mode II components, then in the postbuckling stage the energy-release rate eventually reaches the critical value for delamination growth when the boundary displacement $R\epsilon_o$ becomes sufficiently large.

The ensuing growth of the delamination may or may not require further increase in the boundary displacement. In one case the growth is stable and in the other case it is unstable. Clearly, stability of growth may be determined by examining the change of the energy-release rate with the increase of the delamination radius while maintaining the boundary displacement $R\epsilon_o$ at the value corresponding to the onset of growth. If $\bar{G}$ increases monotonically with increasing $\bar{a}$ under the fixed value of $R\epsilon_o$, the growth of delamination is catastrophic.

Fixing the boundary displacement $R\epsilon_o$ is equivalent to fixing the parameter

$$\epsilon^* \equiv \{12(1-\nu^2)\epsilon_o\}^{1/2}(R/h) \tag{22}$$

Equation (17) implies that

$$\bar{a} = \epsilon^* a/R = \epsilon^* \alpha$$

The dependence of $\bar{G}$ upon $\bar{a}$ for any fixed ϵ^* may be determined from the solid curves in Fig. 4 in the following manner. For any given value of ϵ^*, we draw a broken curve which intersects each solid curve R/a = constant at the unique point $(\bar{a}, \bar{G})$ with the horizontal coordinate $\bar{a} = \epsilon^* a/R$. Such a broken curve shows the dependence of $\bar{G}$ upon the normalized delamination radius $\bar{a}$ under the given value of ϵ^*. It is found that $\bar{G}$ at first increases monotonically with increasing $\bar{a}$ and then decreases slowly at an advanced stage of delamination growth. The slow decrease in $\bar{G}$ is not likely to affect the unstable nature of growth because there is a certain amount of excessive energy release accumulated in the preceding process of delamination growth when $\bar{G}$ exceeded the critical value. This suggests that the growth of a two-dimensional delamination under fixed boundary displacements is generally a catastrophic process. Although a previous analysis of one-dimensional delaminations predicts arrest of growth under certain conditions (Fig. 9 of Ref. 3 contrasts dramatically with Fig. 5 of the present paper), it must be mentioned that the postbuckling solutions of one-dimensional delaminations are rather untypical because the governing von Kármán equations reduce to linear buckling equations with constant coefficients. The solutions of a circular delamination, as given in Tables 1 and 2, show significant nonuniformity of the membrane forces except at the initial stages of postbuckling. The normalized radial force around the center of the delamination eventually becomes tensile. As explained in Ref. 2, this gives rise to enhanced curvature (and bending moment) near the delamination boundary which in turn aggravates the energy-release rate. These interesting features of two-dimensional delaminations are consequences of coupling in the nonlinear postbuckling equations and therefore are not found in the solutions of one-dimensional delaminations. They are also not revealed by recent approximate solutions of circular and elliptical thin-film delaminations subject to uniaxial strain loadings.[9] The latter solutions are based on the Rayleigh–Ritz method with only five undetermined coefficients for the postbuckling deformation. Such solutions cannot reliably predict the membrane forces and bending moments. Nevertheless, they provide

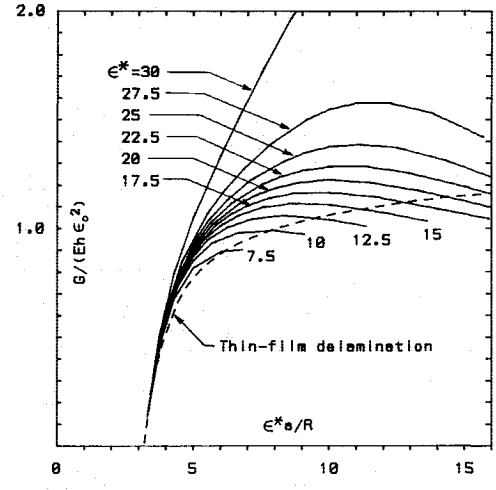

Fig. 5 Energy-release rate vs delamination radius (fixed strain loading).

estimates of global energy-release rates (through numerical differentiation of the total potential energy in an assumed mode of growth) which also indicate rather mild decrease in the later stage of growth.

The broken curves in Fig. 4 are rescaled and replotted in Fig. 5 by introducing a new normalized energy-release rate $\tilde{G}$ with the definition

$$\tilde{G} \equiv \frac{G}{Eh\epsilon_o^2} = \{12(1-\nu^2)\}^2 \frac{\bar{G}}{\tau^5(\epsilon^*)^4} \tag{23}$$

The rescaling of the curves makes the dependence of the energy-release rate upon the delamination radius comparable with the corresponding relation for a thin-film delamination.[2] It is seen that the thin-film approximation generally underestimates the energy-release rate, except when a/R is so large that the delamination spreads over a large portion of the circular plate.

As shown in Fig. 5, the discrepancy in the energy-release rates of the thin-film solutions and the present solutions increases with the parameter ϵ^* and becomes very significant at relatively large strain loading. From Eq. (22), it may be deduced that

$$\frac{\epsilon_o}{\epsilon_p} = \frac{1}{1-\nu}\left(\frac{h\epsilon^*}{3.832\,t}\right)^2$$

where

$$\epsilon_p = \frac{1}{12(1+\nu)}(3.832\,t/R)^2$$

is the buckling membrane strain of a perfect base plate without the delamination. Hence, the error in the energy-release rate arising from the thin-film approximation increases with the strain ratio ϵ_o/ϵ_p. The maximum error as a function of this ratio is in approximate agreement with the results of a similar comparison for one-dimensional delaminations (see Fig. 10 of Ref. 3). (That figure, however, does not explicitly show the error of the thin-film approximation for a given one-dimensional delamination because it compares the maximum energy-release rates of the solutions with and without the thin-film approximation, which occur at different delamination lengths.)

Acknowledgments

This research was supported by a grant from Lockheed Georgia Company to the Georgia Institute of Technology. The authors are indebted to the company for continuous financial support and to John N. Dickson and Sherrill B. Biggers for their encouragement.

References

[1]Kachanov, L.M., "Separation Failure of Composite Materials," *Polymer Mechanics*, Vol. 12, No. 5, Sept.–Oct. 1976, pp. 812–815.

[2]Yin, W.-L., "Axisymmetric Buckling and Growth of a Circular Delamination in a Compressed Laminate," *International Journal of Solids and Structures*, Vol. 21, May 1985, pp. 503–514.

[3]Chai, H., Babcock, C.D., and Knauss, W.G., "One-dimensional Modelling of Failure in Laminated Plates by Delamination Buckling," *International Journal of Solids and Structures*, Vol. 17, No. 11, Nov. 1981, pp. 1069–1083.

[4]Yin, W.-L. and Fei, Z., "Buckling Load of a Circular Plate with a Concentric Delamination," *Mechanics Research Communications*, Vol. 11, No. 5, Nov–Dec. 1984, pp. 337–344.

[5]Yin, W.-L., Sallam, S., and Simitses, G.J., "Ultimate Axial Load Capacity of a Delaminated Plate," *AIAA Journal*, Vol. 24, Jan. 1986, pp. 123–128.

[6]Bodner, S.R., "The Postbuckling Behavior of a Clamped Circular Plate," *Quarterly of Applied Mathematics*, Vol. 12, No. 4, Jan. 1955, pp. 397–401.

[7]Friedrichs, K.O. and Stoker, J.J., "Buckling of the Circular Plate Beyond the Critical Thrust," *Journal of Applied Mechanics*, Vol. 9, No. 1, Mar. 1942, pp. 7–14.

[8]Yin, W.-L. and Wang, J.T.S., "The Energy-release Rate in the Growth of a One-dimensional Delamination," *Journal of Applied Mechanics*, Vol. 51, No. 4, Dec. 1984, pp. 939–941.

[9]Chai, H. and Babcock, C.D., "Two-dimensional Modelling of Compressive Failure in Delaminated Laminates," *Journal of Composite Materials*, Vol. 19, No. 1, Mar. 1985, pp. 67–98.